Oxidative Coupling during Lignin Polymerization Is Determined by Unpaired Electron Delocalization within Parent Phenylpropanoid Radicals

Wendy R. Russell,* Alex R. Forrester,† Andrew Chesson,* and Mark J. Burkitt‡[,1]

*Division of Nutritional Sciences and ‡Division of Biochemical Sciences, Rowett Research Institute, Greenburn Road, Bucksburn, Aberdeen AB21 9SB, United Kingdom; and †Department of Chemistry, University of Aberdeen, Meston Walk, Old Aberdeen AB9 1FX, United Kingdom

The high degree of selectivity observed in the incorporation of phenylpropanoids into lignin may be a consequence of the influence exerted by methoxyl substituents on the ambient radicals generated during biosynthesis. Since unpaired electron distribution may be regarded as an important factor in determining positional selectivity during oxidative coupling, electron spin resonance spectroscopy and Austin Model 1 molecular computation were used to study the effects of methoxyl substitution on unpaired electron distribution in lignin precursor radicals. The data obtained were used to predict the effect of substitution on coupling and were compared with the linkage types observed in complementary dehydrogenation polymerization studies employing each of the lignin precursors. We report that methoxyl substitution increases unpaired electron density on the phenolic oxygen of the precursor phenylpropanoid radicals and that this subsequently determines the nature of the bond formation during polymerization. © 1996 Academic Press, Inc.

Phenylpropanoid oxidative coupling is believed to be the predominant process in lignin biosynthesis and proceeds via a radical mechanism that is catalyzed *in situ* by peroxidases and, possibly, monooxygenases (1, 2). Lignin precursors for this process are generated by the phenylpropanoid pathway in which cinnamic acid is hydroxylated to generate 4-hydroxycinnamic acid, which is in turn progressively methoxylated giving 4-hydroxy-3-methoxycinnamic acid and 4-hydroxy-3,5-dimethoxycinnamic acid (Fig. 1). All of these acids may be reduced via the aldehyde to the corresponding alcohol. In principle, lignin may be formed from any combination of these acids, alcohols, and their intermediates (1, 2), but in practice the polymerization processes appear to involve a high degree of selectivity (3, 4). The relative proportions of the monolignols incorporated into lignin and the nature of the interunit bonding employed, however, vary considerably with cell type, age, and phylogenic origin (5). Typically, the nonmethoxylated 4-hydroxycinnamyl alcohol is detected only in small amounts and in combination with 4-hydroxy-3-methoxycinnamyl alcohol early in the development of the secondary cell wall, whereas the dimethoxylated derivative is found in high concentrations toward the end of the lignification process (6). As a result, heterogeneity of lignin structure appears common, even within a single cell wall (7). The functional significance of the different structural forms of lignin remains unclear.

In the cell walls of grasses, cereals and plants from closely related families, 4-hydroxycinnamic acid and 4-hydroxy-3-methoxycinnamic acid are also incorporated into the lignin structure. Most, if not all, of the 3-methoxylated derivative is ester-bound to cell wall polysaccharide before transport to the wall (8). Once part of the wall, 4-hydroxy-3-methoxycinnamic acid is believed to act as an initiation site for lignification and, in the process, forms a bridge between the polysaccharide to which it was originally linked and the newly formed lignin polymer (9, 10). Similar bridged structures may be formed to a limited extent with 4-hydroxycinnamic acid in some plants, but NMR evidence suggests that the bulk of the nonmethoxylated acid is ester-linked to the primary hydroxyl function of terminal phenylpropanoid units (11).

In reactions involving free radicals, the ability of an

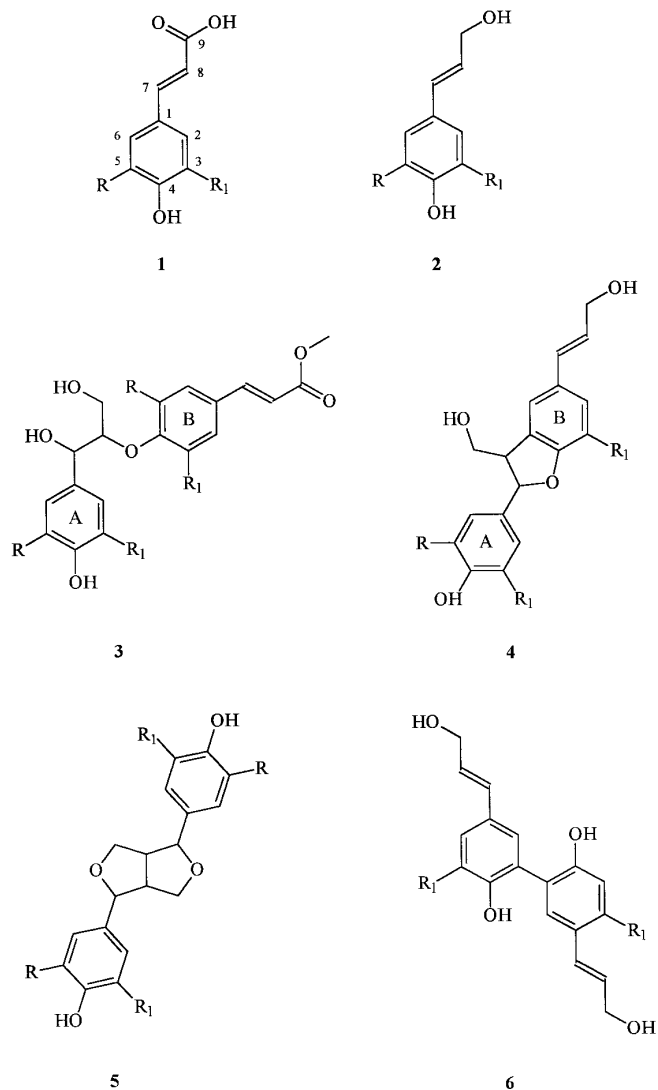[1] To whom correspondence should be addressed. Fax: +44 1224 715349.

FIG. 1. Structures of the substituted cinnamic acids, substituted cinnamyl alcohols, 1a, 4-hydroxycinnamic acid (R and R₁ = H); 1b, 4-hydroxy-3-methoxycinnamic acid (R = H and R₁ = OCH₃); 1c, 4-hydroxy-3,5-dimethoxycinnamic acid (R and R₁ = OCH₃); 2a, 4-hydroxycinnamyl alcohol (R and R₁ = H); 2b, 4-hydroxy-3-methoxycinnamyl alcohol (R = H and R₁ = OCH₃); 2c, 4-hydroxy-3,5-dimethoxycinnamyl alcohol (R and R₁ = OCH₃); and models of the predominant linkages found within lignin, 3a, 8–O–4 (R and R₁ = H); 3b, 8–O–4 (R = H and R₁ = OCH₃); 3c, 8–O–4 (R and R₁ = OCH₃); 4a, 8–5 (R and R₁ = H); 4b, 8–5 (R = H and R₁ = OCH₃); 5a, 8–8 (R and R₁ = H); 5b, 8–8 (R = H and R₁ = OCH₃), 5c, 8–8 (R and R₁ = OCH₃); 6, 5–5 (R₁ = OCH₃).

unpaired electron to delocalize has a significant effect on reactivity and product formation (12). By influencing the delocalization of unpaired electrons in radicals generated on phenylpropanoid lignin precursors by peroxidases, substituent groups would be expected to influence the products of radical coupling reactions and thereby to give purpose to the substrate selection apparently exerted by the plant at different stages in the

lignification process. The purpose of the present study was to determine the effects of the substituent methoxyl groups on unpaired electron delocalization in phenylpropanoid radicals. Phenoxyl radicals were generated using Ce^{IV} as a one-electron oxidant and observed directly using electron spin resonance (ESR) spectroscopy. From comparisons with complementary polymerization product studies, we report that the nature of bond formation during the polymerization of lignin is determined by the pattern of unpaired electron distribution in the phenylpropanoid precursor radicals, which is determined in turn by the pattern of methoxylation in the parent phenylpropanoids.

MATERIALS AND METHODS

General laboratory reagents, cerium(IV) ammonium nitrate, diiso-butylaluminum hydride, substituted 4-hydroxycinnamic acids, and acetophenones were from Aldrich (England). Horseradish peroxidase (Type II) and hydrogen peroxide (27.5% w/v) were from Sigma Chemical Co., Ltd. (England). Reported melting points are uncorrected. Evaporation was under reduced pressure at temperatures not exceeding 40°C. NMR spectra were recorded using a Jeol LA-300 spectrometer (Jeol UK, England), fitted with a 5-mm multinuclear, normal geometry TH5 probe. Operating field for broad band waltz decoupled ^{13}C NMR was 75.4 MHz with a 30° pulse flipping angle (2.4-s pulse width) and 963.4-ms acquisition time. The sweep width employed was 17,000 Hz. Standard DEPT 135 pulse sequences were employed (13). All samples were dissolved in $(CD_3)_2SO$ (0.5 cm^3) containing tetramethylsilane (0.03% v/v) internal reference and run with a probe temperature of 40°C unless otherwise stated. Spectra recorded for polymers (ca. 40,000 scans) were exponentially broadened by a factor of 6.

Preparation of substituted ethyl cinnamates. 4-Hydroxycinnamic acid (16.4 g, 100 mmol), was converted to its ethyl ester by treatment with ethanol (500 cm^3) and acetyl chloride (50 cm^3). After complete disappearance of the acid (16 h) the solvent was removed *in vacuo* and the crude product redissolved in ethyl acetate and extracted with sodium hydrogen carbonate (3% w/v). The organic layer was then left to stand over anhydrous sodium sulfate and filtered and the solvent removed *in vacuo*. Crystallization from ethyl acetate/petroleum ether (bp 40–60°C) gave ethyl 4-hydroxycinnamate (yield 68%): ^{1}H NMR (CD₃OD), 1.1 (t, 3H, CH₂CH₃, J = 7.1 Hz), 4.1 (q, 2H, CH₂CH₃, J = 7.1 Hz), 6.3 (d, 1H, CH=CH, *Jtrans* = 16 Hz), 6.7 (d, 2H, H3, and H5, *Jo* = 8.4 Hz), 7.4 (d, 2H, H2, and H6, *Jo* = 8.4 Hz), 7.6 (d, 1H, CH = CH, *Jtrans* = 16 Hz) ppm. The mono- and dimethoxylated derivatives were prepared in the same manner. Crystallization from ethyl acetate/petroleum ether (bp 40–60°C) gave ethyl 4-hydroxy-3-methoxy cinnamate (yield 74%): ^{1}H NMR (CD₃OD), 1.3 (t, 3H, CH₂CH₃, J = 7.1 Hz), 4.2 (q, 2H, CH₂CH₃, J = 7.1 Hz), 6.3 (d, 1H, CH=CH, *Jtrans* = 16 Hz), 6.8 (d, 1H, H5, *Jo* = 8.2 Hz), 7.1 (d,d, 1H, H6, *Jo* = 8.2 Hz, *Jm* = 1.6 Hz), 7.2 (d, 1H, H2, *Jm* = 1.6 Hz), 7.6 (d, 1H, CH=CH, *Jtrans* = 16 Hz) ppm. Ethyl 4-hydroxy-3,5-dimethoxycinnamate was crystallized from ethyl acetate/petroleum ether (bp 40–60°C), (yield 82%): ^{1}H NMR (CD₃OD), 1.3 (t, 3H, CH₂CH₃, J = 7.1 Hz), 4.2 (q, 2H, CH₂CH₃, J = 7.1 Hz), 3.9 (s, 3H, OCH₃), 6.4 (d, 1H, CH=CH, *Jtrans* = 15.9 Hz), 6.9 (s, 2H, H2, and H6), 7.6 (d, 1H, CH=CH, *Jtrans* = 15.9 Hz) ppm.

Preparation of substituted cinnamyl alcohols. Ethyl 4-hydroxycinnamate (0.36 g, 2.4 mmol) in anhydrous toluene was cooled under nitrogen in an ice-water bath and reduced by treatment with diisobutylaluminum hydride (4.2 eq), added slowly via a dropping funnel over ca. 10 min. The reaction was complete after 1 h at which time it was carefully quenched with ethanol. After partial removal of the

under vacuum at 40°C and addition of water, the product was exhaustively extracted into ethyl acetate. 4-Hydroxycinnamyl alcohol (Fig. 1, 2a) crystallized on evaporation from the dried solvent to give white crystals, mp 88–90.5°C (yield 78%): ^{1}H NMR (CD$_3$OD), 4.1 (d, 2H, CH$_2$OH, J = 5.8 Hz), 6.2 (d,t, 1H, CH=CH, $Jtrans$ = 15.9 Hz, Jv = 5.8 Hz), 6.5 (d, 1H, CH=CH, $Jtrans$ = 15.9 Hz), 6.7 (d, 2H, H2, and H6, Jo = 8.9 Hz), 7.3 (d, 2H, H3, and H5, Jo = 8.9 Hz) ppm; ^{13}C NMR [(CD$_3$)$_2$SO], 61.59 (C9), 115.24 (C3,C5), 127.07 (C8), 127.2 (C2,C6), 127.82 (C1), 128.58 (C7), 156.67 (C4) ppm. The mono- and dimethoxylated cinnamyl alcohols were also prepared by this method. Crystallization from dichloromethane/petroleum ether (bp 40–60°C) gave 4-hydroxy-3-methoxycinnamyl alcohol (Fig. 1, 2b) as pale yellow plates, mp 76.5–78°C (yield 72%): ^{1}H NMR (CD$_3$OD), 4.1 (d, 2H, CH$_2$OH, J = 5.8 Hz), 6.2 (d,t, 1H, CH=CH, $Jtrans$ = 16.1 Hz, Jv = 5.8 Hz), 6.5 (d, 1H, CH=CH, $Jtrans$ = 16.1 Hz), 6.7 (d, 1H, H5, Jo = 8.2 Hz), 6.8 (d,d, 1H, H6, Jo = 8.2 Hz, Jm = 1.8 Hz), 7.0 (d, 1H, H2, Jm = 1.8 Hz) ppm; ^{13}C NMR [(CD$_3$)$_2$SO], 55.65 (OCH$_3$), 61.72 (C9), 109.92 (C2), 115.52 (C5), 119.43 (C6), 127.53 (C8), 128.56 (C1), 129.00 (C7), 146.22 (C3), 147.75 (C4) ppm. Crystallization of 4-hydroxy-3,5-dimethoxycinnamyl (Fig. 1, 2c) was from dichloromethane/petroleum ether (bp 40–60°C) as yellow needles, mp 66.5–68°C (yield 58%): ^{1}H NMR (CD$_3$OD), 3.8 (s, 6H OCH$_3$), 4.2 (d, 2H, CH$_2$OH, J = 5.8 Hz), 6.2 (d,t, 1H, CH=CH, $Jtrans$ = 15.7 Hz, Jv = 5.8 Hz), 6.5 (d, 1H, CH=CH, $Jtrans$ = 15.7 Hz), 6.7 (s, 2H, H2, and H6) ppm; ^{13}C NMR [(CD$_3$)$_2$SO], 56.05 (OCH$_3$), 61.68 (C9), 104.05 (C2,C6), 127.99 (C1), 129.24 (C8), 133.59 (C7), 135.37 (C4), 148.14 (C3,C5) ppm.

Preparation of 8–O–4 models. Methyl 4-[2-hydroxy-2-(4-hydroxyphenol)-1-(hydroxymethyl)ethyl]coumarate (Fig. 1, 3a) was prepared from 4-hydroxyacetophenone (25 mmol) by acetylation in pyridine/acetic anhydride (yield 85%) and conversion to 4-acetoxybromoacetophenone with bromine (1 eq) in CCl$_4$/CHCl$_3$ (yield 53%). The 4-acetoxybromoacetophenone was then added slowly to methyl coumarate treated with K$_2$CO$_3$ in acetone under reflux to give methyl 4-[2-oxo-2-(4-acetoxyphenyl)ethyl]coumarate (yield 94%), which on treatment with K$_2$CO$_3$ in 1,4-dioxane was hydroxymethylated with H$_2$CO (2 eq), (yield 50%). Reduction and concomitant deacetylation was achieved by treatment overnight with NaBH$_4$ in methanol/water. Purification was obtained by flash chromatography on silica (Merck 109385) eluting with CHCl$_3$/ethyl acetate (1/1) (yield 68%): ^{13}C NMR, 51.11 (CO$_2$CH$_3$), 60.12 (A9), 71.08 (A7), 83.86 (A8), 114.42 (B3,B5), 116.12 (A3,A5), 126.24 (B8), 126.60 (B1), 127.66 (A2,A6), 129.70 (B2,B6), 132.27 (A1), 144.25 (B7), 156.28 (B4), 161.23 (A4), 166.82 (B9) ppm. Methyl 4-[2-hydroxy-2-(4-hydroxy-3-methoxyphenyl)-1-(hydroxymethyl)ethyl]ferulate (Fig. 1, 3b): ^{13}C NMR, 51.24 (CO$_2$CH$_3$), 55.54 (BOCH$_3$), 55.86 (AOCH$_3$), 60.28 (A9), 71.08 (A7), 87.55 (A8), 111.24 (B2), 111.46 (B5), 114.11 (A2), 115.24 (A5), 119.11 (B8), 122.58 (A6), 126.85 (B6), 132.40 (B1), 142.91 (B3), 144.68 (B4), 145.58 (B7), 147.04 (A3), 149.70 (A4), 166.96 (B9) ppm and methyl 4-[2-hydroxy-2-(4-hydroxy-3,5-dimethoxyphenyl)-1-(hydroxymethyl)-ethyl]sinapate (Fig. 1, 3c): ^{13}C NMR, 51.34 (CO$_2$CH$_3$), 56.02 (AOCH$_3$), 56.24 (BOCH$_3$), 60.48 (A9), 71.74 (A7), 86.90 (A8), 104.58 (A2,A6), 106.23 (B2,B6), 116.94 (B8), 129.17 (B1), 132.15 (A1), 132.55 (A4), 138.52 (B4), 144.69 (A3,A5), 147.47 (B7), 152.78 (B3,B5), 166.81 (B9) ppm were prepared in similar yields by the same method (14).

Preparation of 8–8 models. The cinnamyl alcohols (Fig. 1, 2a–c) were treated with Ag$_2$O (1.5 eq) in CH$_2$Cl$_2$/water (1/1) (15). Standard processing and purification by flash chromatography on silica (Merck 109385), eluting with CH$_2$Cl$_2$/methanol (95/5) gave the 8–8 dehydrodimers of 4-hydroxycinnamyl alcohol (Fig. 1, 5a) (yield 10%): ^{13}C NMR, 53.46 (C8), 70.61 (C9), 84.87 (C7), 114.90 (C3,C5), 127.29 (C2,C6), 131.52 (C1), 156.59 (C4) ppm; 4-hydroxy-3-methoxycinnamyl alcohol (Fig. 1, 5b) (yield 16%): ^{13}C NMR, 55.35 (C8), 56.12 (OCH$_3$), 72.64 (C9), 85.19 (C7), 110.94 (C2), 116.03 (C5), 118.67 (C6), 133.74 (C1), 147.28 (C4), 149.10 (C3) ppm; and 4-hydroxy-3,5-dimethoxycinnamyl alcohol (Fig. 1, 5c) (yield 22%): ^{13}C NMR, 53.57

(C8), 56.00 (OCH$_3$), 70.98 (C9), 85.23 (C7), 103.72 (C2,C6), 131.42 (C1), 134.90 (C4), 147.80 (C3,C5) ppm.

Preparation of 8–5 models. The 8–5 dehydrodimers were also prepared from the cinnamyl alcohols (Fig. 1, 2a–c) by one-electron oxidation with Ag$_2$O (1.5 eq), the solvent being substituted for CH$_2$Cl$_2$ (anhydrous), which favors 8–5 bond formation (15). Processing and purification by flash chromatography on silica (Merck 109385), eluting with CH$_2$Cl$_2$/methanol (95/5) gave the 8–5 coupled product of 4-hydroxycinnamyl alcohol (Fig. 1, 4a) (yield 18%): ^{13}C NMR, 53.03 (A8), 55.76 (AOCH$_3$), 55.80 (BOCH$_3$), 61.68 (B9), 63.03 (A9), 87.25 (A7), 110.53 (A2), 115.01 (A5), 115.41 (A6), 118.58 (B6), 128.06 (B8), 128.56 (B5), 128.65 (B7), 130.56 (B1), 131.55 (B3), 132.42 (A1), 147.19 (A4), 146.48 (B4), 147.62 (A3) ppm and of 4-hydroxy-3-methoxycinnamyl alcohol (Fig. 1, 4b) (yield 26%): ^{13}C NMR, 52.74 (A8), 61.70 (B9), 63.21 (A9), 86.75 (A7), 108.73 (B3), 115.06 (A3,A5), 122.44 (B2), 127.03 (B6), 127.12 (A2,A6), 127.71 (B8), 128.73 (B5), 128.80 (B1), 129.69 (B7), 132.05 (A1), 158.01 (A4) ppm.

Preparation of 5–5 model. 4-Hydroxy-3-methoxybenzaldehyde (5 g, 32.9 mmol) was 5–5 coupled by treatment with horseradish peroxidase (2025 units) and H$_2$O$_2$ (2.82 cm^3 in 27.5% water) in citrate/phosphate buffer (0.1 mol dm^{-3}, pH 4.2) at 36.5°C (yield 82%) and acetylated by treatment with acetic anhydride and sodium acetate (yield 79%) (16). Condensation of the product (0.5 g, 1.2 mmol) with malonic acid (0.50 g, 4.8 mmol) was achieved in pyridine with aniline (0.04 cm^3) and piperidine (0.04 cm^3) at 55°C for 1 h. The product was precipitated with HCl and crystallized from acetic acid (yield 80%). Conversion to the ethyl ester by treatment at reflux with acetyl chloride in ethanol (yield 51%) and reduction of the product (0.2 g, 0.5 mmol) with diisobutylaluminum hydride (6 cm^3, 1.5 mol dm^{-3} in toluene) gave the 5–5 dehydrodimer of 4-hydroxy-3-methoxycinnamyl alcohol (Fig. 1, 6) (yield 75%): ^{13}C NMR, 55.76 (OCH$_3$), 61.60 (C9), 107.88 (C2), 115.25 (C5), 121.75 (C8), 126.00 (C6), 127.10 (C1), 127.40 (C7), 129.21 (C4), 148.10 (C3) ppm.

Preparation of dehydrogenation polymers (zutropfverfahren). 4-Hydroxycinnamyl alcohol (130 mg, 0.56 mmol) was dissolved in phosphate buffer (88 cm^3, pH 6.5, 25 mmol dm^{-3}) to give solution A. Solution B was prepared by dissolving hydrogen peroxide (0.076 cm^3, 0.67 mmol, 1.2 eq) in phosphate buffer (88 cm^3, pH 6.5, 25 mmol dm^{-3}). Both A and B were added to a solution of horseradish peroxidase (275 units, 2.4 mg) in phosphate buffer (24 cm^3, pH 6.5, 25 mmol dm^{-3}) at a rate of 2 cm^3 h^{-1} under nitrogen with continuous stirring. After 24 h a further aliquot of peroxidase was added (125 units, 1.1 mg). After 48 h the precipitate was filtered on a 0.45-μm membrane, resuspended in water, and again filtered and thoroughly washed. A grayish powder (yield 62%) was obtained on freeze drying. Dehydrogenation polymers containing 4-hydroxy-3-methoxycinnamyl alcohol (beige powder, yield 62%) and 4-hydroxy-3,5-dimethoxy cinnamyl alcohol (orange powder, 32%) were also prepared.

Preparation of dehydrogenation polymers (zulaufverfahren). 4-Hydroxycinnamyl alcohol (130 mg, 0.56 mmol) was dissolved in phosphate buffer (200 cm^3, pH 6.5, 25 mmol dm^{-3}) along with horseradish peroxidase (275 units, 2.4 mg). While being continuously stirred under nitrogen, hydrogen peroxide (0.076 cm^3, 0.67 mmol, 1.2 eq) was added and the reaction mixture left stirring for 24 h. The precipitate was filtered on a 0.45-μm membrane, resuspended in water, and again filtered and thoroughly washed. A pale grayish powder (yield 78%) was obtained on freeze drying. Dehydrogenation polymers containing 4-hydroxy-3-methoxycinnamyl alcohol (pale beige powder, yield 68%) and 4-hydroxy-3,5-dimethoxycinnamyl alcohol (pale orange powder, yield 30%) were also prepared.

Radical generation and ESR spectroscopy. Radicals were generated in a two-stream ESR flow cell (Bruker UK, England), positioned in the cavity of a Bruker E106 spectrometer, via the continuous mixing of substrate (10^{-2} mol dm^{-3} in 50% v/v methanol) and ammonium cerium(IV) nitrate (10^{-3} mol dm^{-3} in 0.25 mol dm^{-3} sulfuric acid) solutions. Flow was maintained using a Watson–Marlow Flow 505S/RL pump (Watson–Marlow, Ltd., England) placed before the
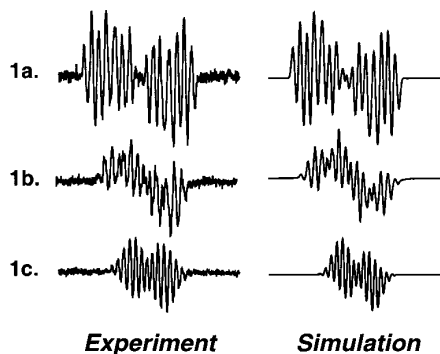
FIG. 2. ESR spectra and computer-simulated spectra of radicals obtained from hydroxycinnamic acids. 1a, 4-hydroxycinnamic acid; 1b, 4-hydroxy-3-methoxycinnamic acid; 1c, 4-hydroxy-3,5-dimethoxycinnamic acid. The simulation of spectrum 1b contains a broad signal from a polymer-derived radical. The hyperfine coupling constants of the radicals are given in Table I.

cell and producing a combined flow rate of 4.8 cm^3 s^{-1}. The postreaction pH values were measured using a meter (Corning, United Kingdom; Model 220) positioned in the output stream from the ESR cell and were typically 0.5–1.5. Spectra (X-band) were recorded using the following instrument settings: modulation frequency, 100 kHz; center field, 3479 Gauss; sweep width, 40 Gauss; modulation amplitude, 0.8 Gauss; time constant, 41 ms; sweep time 90 s; power, 20 mW; and a suitable receiver gain setting (typically 6.3×10^4).

Spectral simulation and computation of unpaired electron spin density. Computer simulations of spectra, giving the hydrogen hyperfine coupling constants (a_H), were performed using the SIM-EPR program, which sequentially varies all the parameters for each radical species until a minimum in the error surface is located (17). Goodness-of-fit was determined by visual comparison and as a minimum in the sum of the squared residuals. The density of the unpaired electron (ρ) at each carbon atom was calculated from the hyperfine coupling constants using the McConnell relationship, $a_H = \rho Q$ (18), in which Q is the proportionality factor (see below) (19). The unpaired electron density on the ESR-silent positions was then calculated by difference. Graphical plots of spin density and numerical values for the α and β electrons were obtained by a quantum mechanical method using the HyperChem molecular simulation program (20, 21). *Ab initio* methods were not feasible due to the size of the molecules and the requirement for a large basis set; therefore, the semiempirical method Austin Model 1 (AM1)[2] was selected (22, 23). AM1 molecular orbital calculations have been demonstrated to support spin density values derived from ESR hyperfine coupling constants (24).

RESULTS AND DISCUSSION

ESR spectra were observed following the one-electron oxidation of various phenylpropanoid lignin precursor cinnamic acids (Fig. 2) and cinnamyl alcohols (Fig. 3). Hyperfine coupling constants were determined directly from the experimental spectra by computer simulation (Figs. 2 and 3, Table I). Although the probability of unpaired electron spin density at the nucleus is zero, hyperfine coupling to proton and other nuclei

[2] Abbreviation used: AM1, Austin Model 1.

can be observed by ESR due to spin polarization. Proton coupling results from spin polarization of the valence electron of the hydrogen atom with the unpaired electron. According to the McConnell relationship, $a_H = \rho Q$, the hyperfine coupling constant (a_H) to a proton is proportional to the density of the unpaired electron (ρ) on the carbon atom to which it is directly bound (18). The proportionality factor, Q, varies depending on the environment of the unpaired electron and lies between 20 and 30 Gauss. In this study, a Q value of 22.5 Gauss was used, which is considered to be the best estimate assuming the value is constant for all the C–H bonds (20). In a given radical, the Q value for neutral carbon atoms can vary within a range of approximately 10%. In this study, since similar compounds were compared, and because any contribution resulting from the small numerical differences would remain constant between the parent radicals, the value of Q was allowed to remain constant. Applying the McConnell relationship with a Q value of 22.5 Gauss, spin density values were obtained for each carbon center in the radicals observed. However, polarization is not accounted for and therefore it is not possible to distinguish between positive and negative spin density (i.e., α and β electrons). Positive and negative spin densities were distinguished using computational methods available to calculate the theoretical total spin density ($\alpha - \beta$). Geometry optimization was performed to achieve the equilibrium structures by entering approximate structures into the HyperChem molecular simulation program (21, 22). The semiempirical method AM1 was then selected (23, 25), which is an altered version of the modified neglect of the differential overlap method (26, 27) in which many of the approximations are similar but the overall accuracy of the method is significantly improved. Compensation for the radical center was achieved by deletion of the phenoxyl hydrogen and setting the specific
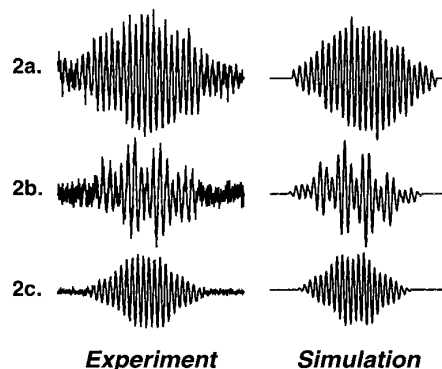

FIG. 3. ESR spectra and computer-simulated spectra of radicals obtained from hydroxycinnamyl alcohols. 2a, 4-hydroxycinnamyl alcohol; 2b, 4-hydroxy-3-methoxycinnamyl alcohol; 2c, 4-hydroxy-3,5-dimethoxycinnamyl alcohol. The hyperfine coupling constants of the radicals are given in Table I.

TABLE I

ESR Hyperfine Coupling Constants (a_H) for Radicals[a] Generated from
Hydroxycinnamic Acids and Hydroxycinnamyl Alcohols

	$a_{H(2)}$	$a_{H(3)}$	$a_{H(5)}$	$a_{H(6)}$	$a_{H(7)}$	$a_{H(8)}$	$a_{H(9)}$	$a_{H(OMe)}$
1a	1.68	5.26	5.65	1.68	3.06	6.36	—	—
1b	1.53	—	5.56	1.70	2.64	5.28	—	1.69
1c	0.95	—	—	1.26	1.69	4.82	—	1.33
2a	1.41	4.97	5.36	1.17	2.57	6.40	4.31	—
2b	1.16	—	5.33	1.86	2.32	5.50	3.92	1.38
2c	1.18	—	—	1.11	1.39	5.89	4.78	1.15

[a] Radicals were generated via oxidation with Ce^{IV} in a two-stream fast-flow system, as described under Materials and Methods. Hyperfine coupling constants (in Gauss) were measured directly from the observed spectra and optimized by computer simulation (Figs. 1 and 2). The structures of the parent compounds are shown in Fig. 1. 1a, 4-hydroxycinnamic acid; 1b, 4-hydroxy-3-methoxycinnamic acid; 1c, 4-hydroxy-3,5-dimethoxycinnamic acid; 2a, 4-hydroxycinnamyl alcohol; 2b, 4-hydroxy-3-methoxycinnamyl alcohol; 2c, 4-hydroxy-3,5-dimethoxycinnamyl alcohol.

charge to 0 and spin multiplicity to 2. An unrestricted Hartree−Fock wave function was then selected to allow for the unpaired electron. Once optimized, a single point calculation employing AM1 was performed to give a graphical distribution of the total spin density with the *x* axis aligned with the primary structure (Fig. 4). This plot of unpaired electron density is directly comparable to the measured ESR hyperfine coupling constants (Table I). Having determined the sign by computational methods, summation overall gives an unaccounted value for each lignin precursor which follows a general trend for each series (Fig. 5). This value indicates the delocalization of the radical to the non-carbon nuclei and ESR-silent positions in each radical. In general, these values are best regarded only to an order of magnitude, as the *Q* values are approximated and the McConnell equation has its own limitations. However, similar compounds differing only in their degree of substitution can be compared with confidence. To investigate the effect of the ESR-silent positions on the overall electron spin population, the theoretical distribution of the unpaired α-electron for each of the precursor radicals was calculated. This was achieved by obtaining values for both the α and the β electrons from log files within the HyperChem program collected during single-point AM1 calculations. Summation $(\alpha - \beta)$ provided values for spin density within each orbital and therefore the overall unpaired electron distribution. Although all the spectroscopically blind positions (with the exception of the phenolic oxygen) are not available for coupling, the spin densities on the carbon-centered atoms have a significant effect on the overall α-electron distribution. From these values the percentage α-electron on the phenoxyl radical was calculated (Table II) and shows that the contribution from the spin density on phenolic oxygen accounts for only 23–47% of the total spin density not accounted for by ESR.

The inability to isolate lignin in its natural state has

prompted the development of methods to polymerize monolignols *in vitro*. Although such structural representations of higher molecular mass models can differ substantially from native lignin, the use of dehydrogenation polymers is extremely valuable when probing the mechanism of incorporation of different precursors (28). As polymerization occurs, structural variations are dependent on the static concentration of radicals and the species of monolignol present. Two procedures are reported for synthesis, of which the *zutropfverfahren* (drop method) is the most successful in yielding a high molecular weight product most closely resembling lignin (28, 29). This method requires the addition of separate solutions of the substrate and hydrogen peroxide simultaneously and slowly to a buffered solution of the enzyme. In the second method, the *zulaufverfahren* (mixing method), the substrate and oxidant are added together in one addition. Both methods of polymerization were employed in the present study. Interpretation of the NMR spectra (Fig. 6 and Table III) was made by comparison with both published data (30, 31) and model compounds which were synthesized to contain each specific linkage type (Fig. 1). *Zulaufverfahren* polymerization of all three monolignols resulted in predominantly 8–5 (Fig. 1, 4) and 8–8 (Fig. 1, 5) coupling for substrates with unsubstituted *ortho* positions. Only for the 4-hydroxy-3,5-dimethoxycinnamyl alcohol polymer were 8−O−4 linkages (Fig. 1, 3) distinguishable. This type of polymerization represents monolignol coupling in the presence of a high concentration of monomeric radicals and tends to produce low molecular weight fragments due to initial coupling to dimers followed by further polymerization which successively lowers the reactivity of the radical species, resulting in eventual termination.

By maintaining the radical concentration at a steady and low state as in *zutropfverfahren* polymerization, there are more monomer−monomer coupling reactions,
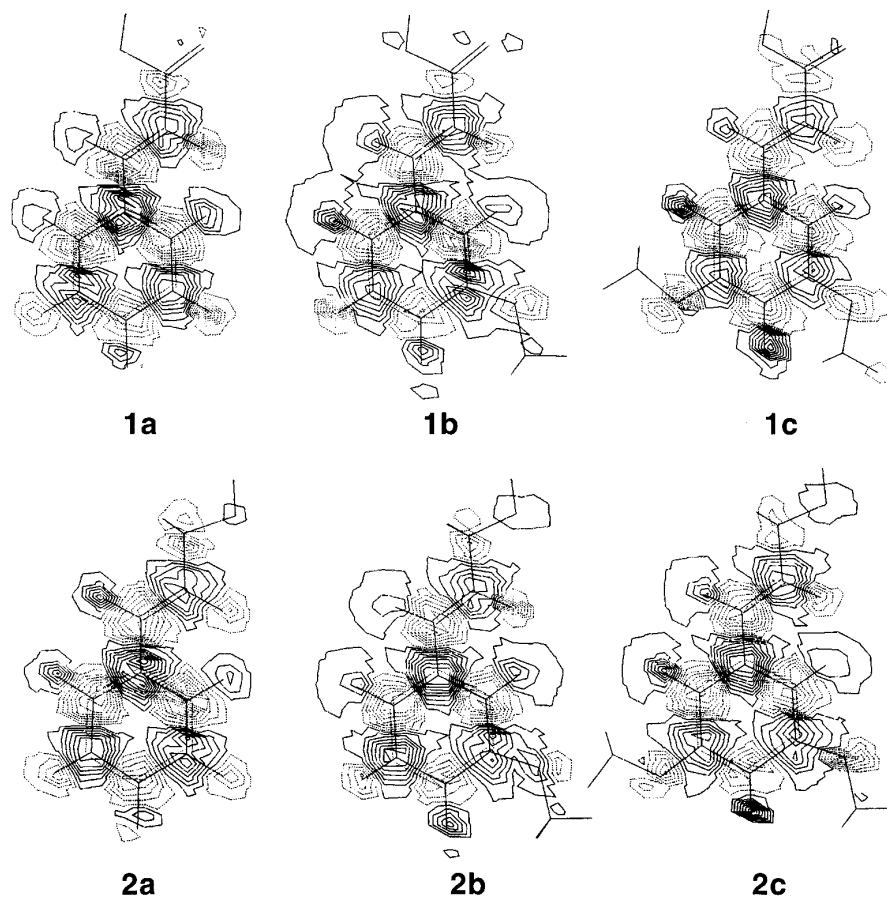
FIG. 4. Plot of total unpaired electron spin density calculated for the geometrically optimized structures of phenylpropanoid radicals obtained using the Austin Model 1 on HyperChem. The *x* axis is aligned with the primary structure and positive spin densities are represented by intact lines. 1a, 4-Hydroxycinnamic acid; 1b, 4-hydroxy-3-methoxycinnamic acid; 1c, 4-hydroxy-3,5-dimethoxycinnamic acid; 2a, 4-hydroxy-cinnamyl alcohol; 2b, 4-hydroxy-3-methoxycinnamyl alcohol; 2c, 4-hydroxy-3,5-dimethoxycinnamyl alcohol.

resulting in higher molecular weight polymers. This process reflects the intrinsic electronic delocalization of the monolignol precursor, and the products demonstrate a higher resemblance to lignins produced *in vivo*. The main features observed from the products of *zutropfverfahren* polymerization were the decrease in resonances due to the 8–8 linkage for the 4-hydroxy-3,5-dimethoxycinnamyl alcohol polymer (Fig. 1, 5) and the incomplete saturation of the exocyclic double bond, showing the nonparticipation of some C8 positions within this polymer. The 8–8 linkage (Fig. 1, 5) has been shown to be the predominant mode of bonding in dilignols of this species (1) and also when there is a high concentration of monomeric radicals present, as for *zulaufverfahren* polymerization. The signal assignments indicate a high degree of 8–O–4 bonding (Fig. 1, 3). This can be rationalized by consideration of the ESR hyperfine coupling constants which suggest that, for positions available for coupling, a large amount of the unpaired electron density is present on the oxygen

atom. Therefore, under conditions which favor monomer–monomer coupling, (i.e., steady flow and low concentration of radicals), the phenoxyl radical should be involved in bonding. Due to the reversible nature of O–O coupling, peroxide linkages are unstable; therefore, the most available site for coupling to the phenoxyl radical is with C8, accounting for the predominant formation of the 8–O–4 linkage (Fig. 1, 3). The polymer resulting from 4-hydroxy-3-methoxycinnamyl alcohol (Fig. 1, 2b) contained primarily 8–5 (Fig. 1, 4) and 8–8 (Fig. 1, 5) linkages, with possibly a small contribution from 8–O–4 linkages (Fig. 1, 3). This is consistent with the spin densities at positions C5, C8, and the phenoxyl oxygen (Fig. 4 and Table II). The polymer formed from 4-hydroxycinnamyl alcohol (Fig. 1, 2a) consisted of primarily 8–8 bonding (Fig. 1, 5). Also evident were 8–5 linkages (Fig. 1, 4), but in smaller quantities than found in the 4-hydroxy-3-methoxycinnamyl alcohol polymer, which had only one unsubstituted *ortho* position. The preference of 4-hydroxycinnamyl alcohol (Fig.
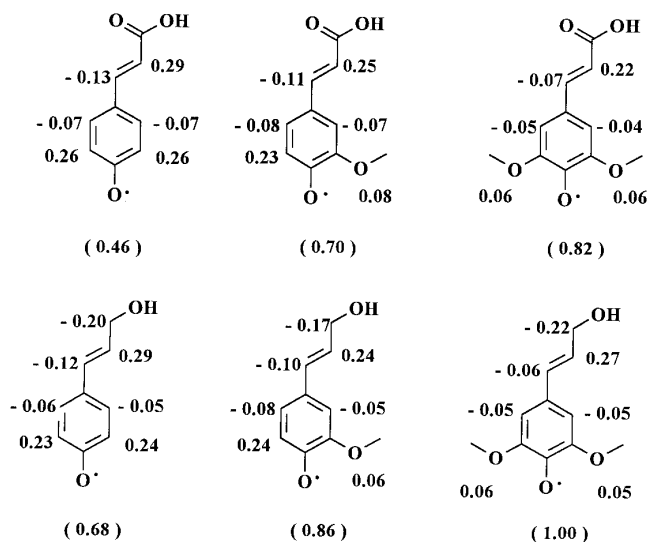
FIG. 5. Unpaired electron spin density at the carbon nuclei of phenylpropanoid radicals calculated from ESR spectra (Figs. 2 and 3) using the McConnell equation with $Q = 22.5$ (see Materials and Methods). The signs were calculated computationally using Austin Model 1 on HyperChem (see Fig. 4). The value for the spin density not accounted for by ESR is given in parentheses.

1, 2a) to form 8–8 (5) and 8–5 (4) linkages, rather than 8–O–4 (3), is unusual because the thermodynamic barrier imposed by methoxyl substitution and favoring 8–8 bonding (5) in disubstituted monolignols is lifted. Control of this mechanism may therefore be kinetic and can be rationalized by the spin density results which indicated that the combined proportion of time spent at the carbon nuclei was greater than the indicated value for electron spin density on the oxygen (Fig. 1 and Table II). The generally low spin density on the phenoxyl oxygen may account for the predominant involvement of C8 in the synthetic oxidative coupling experiments.

The regiochemical association of 4-hydroxy-3-methoxycinnamic acid (Fig. 1, 1b) to function as a cross-linking agent between polysaccharides and polyphenolics has received considerable attention (32, 33). Cross-linking is facilitated by the ability of 4-hydroxy-3-methoxycinnamic acid (Fig. 1, 1b) to form both ester and ether linkages. Although this property is shared by the non- (Fig. 1, 1a) and dimethoxylated (1c) cinnamic acids, bridging appears to be restricted to the monomethoxylated compound (1b). The reason for the selection of 4-hydroxy-3-methoxycinnamic acid (Fig. 1, 1b) over 4-hydroxy-3,5-dimethoxycinnamic acid (1c) is not known. However, it might relate to the later expression of enzymes responsible for the hydroxylation and methylation of 4-hydroxy-3-methoxycinnamic acid (1b) and to the consequential nonavailability of the dimethoxylated substrate during early stages of wall development.

The nonmethoxylated 4-hydroxycinnamic acid (Fig. 1, 1a) is found in small amounts esterified to arabinoxylans during primary cell wall formation and more extensively to lignin in the later stages of development (32–36), where it has been shown to be esterified exclusively by reaction with the primary hydroxyl on lignin side chains (11). Despite the possibility of subsequent reactions with monolignols, esterified 4-hydroxycinnamate does not appear to participate in further oxidative coupling (11). Spin density measurements revealed the distribution of the unpaired electron on the carbon nuclei to be greater for the nonmethoxylated acid (Fig. 1, 1a), predicting a preference for C–C bond formation, which was indeed observed in the polymerization experiments. This high degree of C–C bonding was also demonstrated by the structure of the 4-hydroxycinnamyl alcohol polymer and its resistance when treated at high temperature with sodium hydroxide (data not shown). In the later stages of lignification 4-hydroxy-3,5-dimethoxycinnamyl alcohol (Fig. 1, 2c) is the predominant alcohol present. Due to deactivation of 4-hydroxycinnamate radicals by delocalization, coupling with the dimethoxylated alcohol is essentially prevented. This allows the competing 8–O–4 polymerization of the dimethoxylated alcohols to proceed. The esterified 4-hydroxycinnamic acid can be seen as a terminal unit. This function would be less readily fulfilled by 4-hydroxy-3-methoxycinnamic acid (Fig. 1, 1b) and 4-hydroxy-3,5-dimethoxycinnamic acid (1c) since the increased electron density on the phenolic oxygen, for the these acids, would allow further development of the lignin molecule to occur.

The temporal sequence of monolignol production observed in most plants, in which the nonmethoxylated (Fig. 1, 2a) and monomethoxylated (2b) lignin precursors are replaced by the dimethoxylated lignol (2c) (6), results in a spatial distribution of lignins with a different composition within the wall. Antibody probes

TABLE II

Theoretical Values[a] for the Percentage Unpaired α-Electron Occupying Orbitals on the Phenolic Oxygen

	% unpaired α-electron
1a	16.05
1b	23.54
1c	38.74
2a	15.54
2b	22.81
2c	36.82

[a] Values calculated by AM1 method (see Results and Discussion) for 1a, 4-hydroxycinnamic acid; 1b, 4-hydroxy-3-methoxycinnamic acid; 1c, 4-hydroxy-3,5-dimethoxycinnamic acid; 2a, 4-hydroxycinnamyl alcohol; 2b, 4-hydroxy-3-methoxycinnamyl alcohol; and 2c, 4-hydroxy-3,5-dimethoxycinnamyl alcohol.
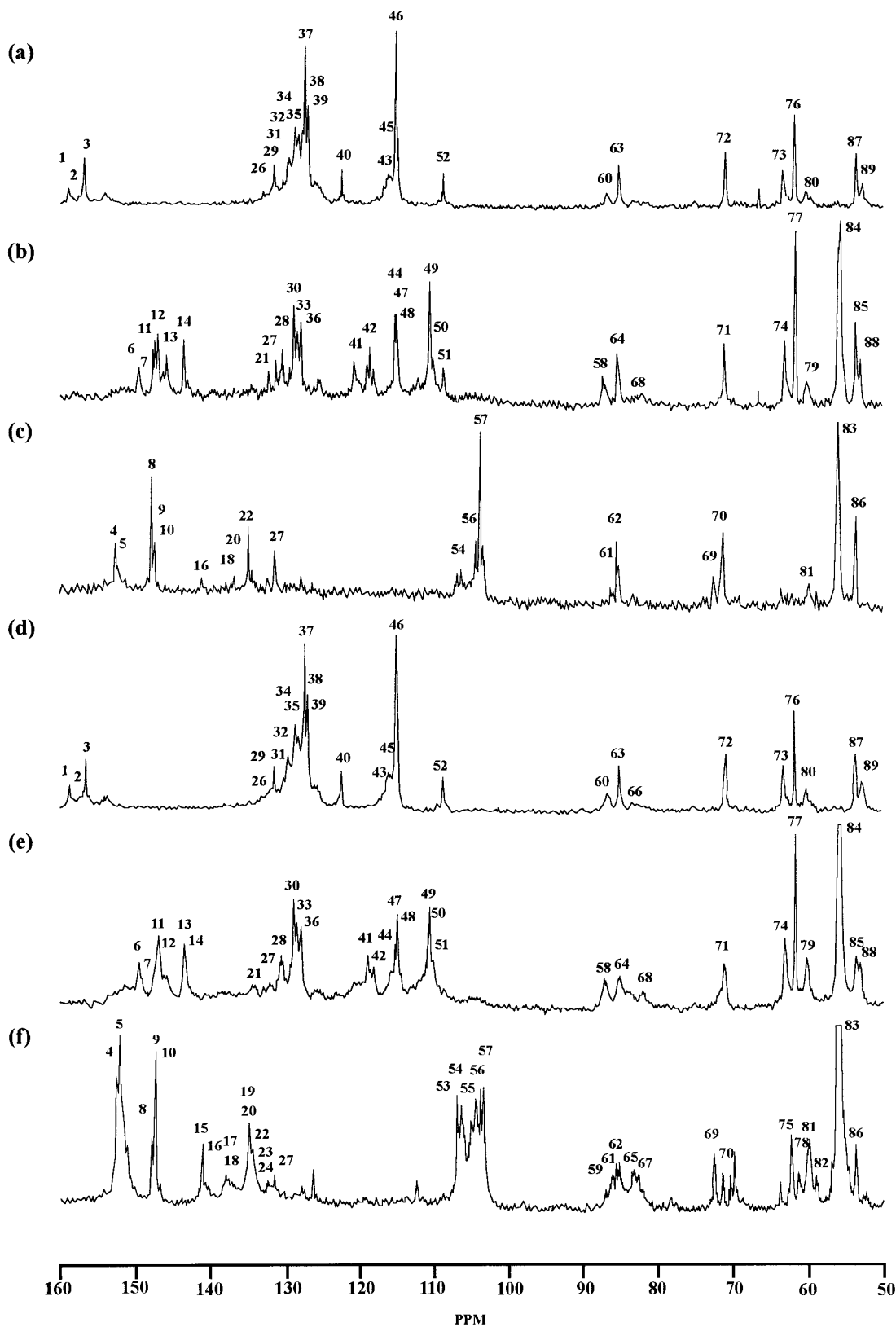
FIG. 6. ^{13}C NMR spectra (50–160 ppm region) of dehydrogenation polymers. *Zulaufverfahren* polymers: (a) 4-hydroxycinnamyl alcohol, (b) 4-hydroxy-3-methoxycinnamyl alcohol, (c) 4-hydroxy-3,5-dimethoxycinnamyl alcohol. *Zutropfverfahren* polymers: (d) 4-hydroxycinnamyl alcohol, (e) 4-hydroxy-3-methoxycinnamyl alcohol, (f) 4-hydroxy-3,5-dimethoxycinnamyl alcohol.

TABLE III

Assignments for ^{13}C Spectra of Dehydrogenation Polymers[a]

Signal	Assignment	ppm	Signal	Assignment	ppm
1	A 8−5 (B4)	158.80	46	A 8−8 (C3, C5)*	115.03
2	A 8−5 (A4)	156.77	47	B 8−8 (C5)*	115.02
3	A 8−8 (C4)	156.70	48	B 8−5 (A5)	115.02
4	C 7,8−O−4 (B3, B5)	152.59	49	B 8−8 (C2)*	110.61
5	C 8−O−4 (B3, B5)	152.20	50	B 8−5 (A2)*	110.61
6	B 8−5 (A4)	149.73	51	B 8−5 (B2)*	110.12
7	B 8−8 (C3)	149.39	52	A 8−5 (B3)*	108.74
8	C 8−8 (C3, C5)	147.93	53	C 7,8−O−4 (B2, B6)*	106.97
9	C 7,8−O−4 (A3, A5)	147.47	54	C 8−O−4 (B2, B6)*	106.39
10	C 8−O−4 (A3, A5)	147.47	55	C 7,8−O−4 (A2, A6)*	105.03
11	B 8−5 (A3)	147.14	56	C 8−O−4 (A2, A6)*	104.30
12	B 8−5 (B4)	146.46	57	C 8−8 (C2, C6)*	103.77
13	B 8−8 (C4)	145.98	58	B 8−5 (A7)*	87.00
14	B 8−5 (B3)	143.72	59	C 7,8−O−4 (A8)*	86.81
15	C 7,8−O−4 (B4)	141.15	60	A 8−5 (A7)*	86.59
16	C 8−O−4 (B4)	141.15	61	C 8−O−4 (A8)*	85.98
17	C 7,8−O−4 (A4)	134.98	62	C 8−8 (C7)*	85.43
18	C 8−O−4 (A4)	134.98	63	A 8−8 (C7)*	85.01
19	C 7,8−O−4 (A1)	134.47	64	B 8−8 (C7)*	84.94
20	C 8−O−4 (A1)	134.47	65	C 7,8 saturated (C7)*	83.26
21	B 8−5 (A1)	134.27	66	A 7,8 saturated (C7)*	83.24
22	C 8−8 (C4)	134.09	67	A 7,8−O−4 (A7)*	82.44
23	C 7,8−O−4 (B1)	132.48	68	B 7,8 saturated (C7)*	81.88
24	C 8−O−4 (B1)	132.49	69	C 8−O−4 (A7)*	72.32
25	B 8−8 (C1)	132.25	70	C 8−8 (C9)**	71.26
26	A 8−5 (A1)	131.60	71	B 8−8 (C9)**	71.05
27	C 8−8 (C1)	131.52	72	A 8−8 (C9)**	70.86
28	B 8−5 (B1)	130.67	73	A 8−5 (A9)**	63.18
29	A 8−8 (C1)	130.36	74	B 8−5 (A9)**	63.02
30	B 8−5 (B7)*	129.99	75	C 8−O−4 (B9)**	62.05
31	A 8−5 (B1)	129.65	76	A 8−5 (B9)**	61.67
32	A 8−5 (B7)*	128.80	77	B 8−5 (B9)**	61.67
33	B 8−5 (B5)	128.59	78	C 7,8 saturated (C9)**	61.15
34	A 8−5 (B5)*	128.48	79	B 7,8 saturated (C9)**	60.17
35	A 8−5 (B8)*	128.32	80	A 7,8 saturated (C9)**	60.12
36	B 8−5 (B8)*	128.10	81	C 8−O−4 (A9)**	59.73
37	A 8−8 (C2, C6)*	127.42	82	C 7,8−O−4 (A9)**	58.79
38	A 8−5 (A2, A6)*	127.42	83	C OCH$_3$*	55.91
39	A 8−5 (B6)*	127.10	84	B OCH$_3$*	55.82
40	A 8−5 (B2)*	122.42	85	B 8−8 (C8)*	53.69
41	B 8−8 (C6)*	119.07	86	C 8−8 (C8)*	53.62
42	B 8−5 (B6)*	118.26	87	A 8−8 (C8)*	53.59
43	A 8−5 (A3)	116.16	88	B 8−5 (A8)*	53.10
44	B 8−5 (A6)*	115.78	89	A 8−5 (A8)*	52.73
45	A 8−5 (A5)*	115.71			

[a] Polymers were prepared as described under Materials and Methods. Assignments from Fig. 6 are for polymers derived from 4-hydroxycinnamyl alcohol, A; 4-hydroxy-3-methoxycinnamyl alcohol, B; and 4-hydroxy-3,5-dimethoxycinnamyl alcohol, C. From DEPT experiment, *, 1° and 3° carbons; **, 2° carbons; and all other signals are for quaternary carbons.

raised against 4-hydroxycinnamyl alcohol (Fig. 1, 2a) have confirmed earlier autoradiography studies that nonmethoxylated units are restricted to the earliest sites of lignification in the middle lamella (37, 38). Those raised against the 4-hydroxy-3-methoxy dehydrogenation polymer are more generally distributed but show very limited reactivity, suggesting that binding epitope(s) are not readily available (37). In contrast, antibodies prepared with a mixed dehydrogenation polymer formed from the mono- (Fig. 1, 2b) and dimethoxylated (2c) lignols are highly active, particularly in the secondary wall layers, the last region of the wall to become lignified (38). Our spin density measurements suggest that a consequence of this temporal sequence would be a transition in lignin structure from a preponderance of 8−8 (Fig. 1, 5) and 5−5 (6) bonding in the

middle lamella, through lignin with an approximately equal proportion of 8–5 (4), 8–8 (5) and 8–O–4 (3) linkages in the primary wall layer to the secondary wall which would consist largely of 8–O–4 (3) bonded monolignols with fewer C–C linkages. The flexibility of macromolecules is the most important characteristic, predicting the property of polymers. The rigidity of lignin is associated with its topotactic geometry and intermolecular interactions, and the use of theoretical models has shown that 8–O–4 bonding (Fig. 1, 3) would allow the closest packing of molecules within lignin (39). This conformation is stabilized by sandwich-type stacking of the planar aromatic rings. However, while the spin density results and information from dehydrogenation polymer formation and modeling may account for the formation of different lignins within a cell wall, the benefit to the plant in structural or physiological terms has yet to be identified.

ACKNOWLEDGMENTS

REFERENCES

1. Sarkanen, K. V. (1971) *in* Lignins: Occurrence, Formation, Structure and Reactions (Sarkanen, K. V., and Ludwig, C. H., Eds.), pp. 95–163, Wiley–Interscience, New York.

2. McDougall, G. J., Stewart, D., and Morrison, I. M. (1994) *Planta* 194, 9–14.

3. He, L., and Terashima, N. (1989) *Mokuzai Gakkaishi* 35, 116–122.

4. Erickson, M., Miksche, G. E., and Somfai, I. (1973) *Holzforschung* 27, 113–119.

5. Monties, B. (1985) *Annu. Proc. Phytochem.* 5, 161–181.

6. Terashima, N., Fukushima, K., He, L-F., and Takabe, K. (1993) *in* Forage Cell Wall Structure and Digestibility (Jung, H. G., Buxton, D. R., Hatfield, R. D., and Ralph, J., Eds.), pp. 247–270, ASA-CSSA-SSSA, Madison, WI.

7. Lapierre, C., Polet, B., and Monties, B. (1991) *Phytochemistry* 30, 659–662.

8. Myton, K. E., and Fry, S. C. (1994) *Planta* 193, 326–330.

9. Lam, T. B. T., Iiyama, K., and Stone, B. A. (1992) *Phytochemistry* 31, 1179–1183.

10. Lam, T. B. T., Iiyama, K., and Stone, B. A. (1994) *Phytochemistry* 37, 327–333.

11. Ralph, J., Hatfield, R. D., Quideau, S., Helm, R. F., Grabber, J. H., and Jung, H. J. G. (1994) *J. Am. Chem. Soc.* 116, 9448–9456.

12. Pankratov, A. N. (1994) *J. Mol. Struct. (THEOCHEM)* 315, 179–186.

13. Bendall, M. R., Pegg, D. T., Doddrell, D. M., and Thomas, D. M. (1982) *J. Magn. Reson.* 46, 43–53.

14. Helm, R. F., and Ralph, J. (1992) *J. Agric. Food Chem.* 40, 2167–2175.

15. Quideau, S., and Ralph, J. (1992) *Holzforschung* 40, 12–22.

16. Baumgartner, J., and Neukom, H. (1972) *Chimia* 26, 366–368.

17. Duling, D. R. (1994) *J. Magn. Reson.* 104B, 105–110.

18. McConnell, H. M. (1956) *J. Chem. Phys.* 24, 460–467.

19. McLachlan, A. D. (1960) *Mol. Phys.* 3, 233–252.

20. Weissman, S. I., Tuttle, T. R., and De Boer, E. (1957) *J. Chem. Phys.* 61, 28–31.

21. Froimowitz, M. (1993) *Biotechniques* 14, 1010–1013.

22. Pazun, J. L. (1993) *J. Chem. Inf. Comput. Sci.* 33, 931–933.

23. Aleman, C., Vega, M. C., and Perez, J. J. (1993) *J. Mol. Struct.* 282, 251–258.

24. Samoilova, R. I., van Liemt, W., Steggerda, W. F., Lugtenburg, J., Hoff, A. J., Spoyalov, A. P., Tyryshkin, A. M., Gritzan, N. P., and Tsvetkov, Y. D. (1994) *J. Chem. Soc. Perkins* 2, 609–614.

25. Aleman, C., Vega, M. C., and Perez, J. J. (1993) *J. Mol. Struct.* 281, 39–44.

26. Dewar, M. J. S. (1962) The Molecular Orbital Theory of Organic Chemistry, McGraw–Hill, New York.

27. Dewar, M. J. S., and Thiel, W. (1977) *J. Am. Chem. Soc.* 99, 4899–4907.

28. Freudenberg, K., and Neish, A. C. (1968) Constitution and Biosynthesis of Lignin, Springer-Verlag, Berlin/Heidelberg/New York.

29. Freudenberg, K. (1963) *Chem. Ber.* 96, 1844–1848.

30. Quideau, S., and Ralph, J. (1992) *Holzforschung* 48, 124–132.

31. Xie, Y., Yasuda, S., and Terashima, N. (1994) *Mokuzai Gakkaishi* 40(2), 191–198.

32. Ralph, J., and Helm, R. F. (1993) *in* Forage Cell Wall Structure and Digestibility (Jung, H. G., Buxton, D. R., Hatfield, R. D., and Ralph, J., Eds.), pp. 201–246, ASA-CSSA-SSSA, Madison, WI.

33. Lam, T. B. T., Iiyama, K., and Stone, B. A. (1992) *Phytochemistry* 31, 2655–2658.

34. Mueller-Harvey, I., Hartley, R., Harris, P. J., and Curzon, E. H. (1986) *Carbohydr. Res.* 148, 71–85.

35. Scalbert, A., Monties, B., Lallemand, J. Y., Guittet, E., and Rolando, C. (1985) *Phytochemistry* 24, 1359–1362.

36. Atushi, K., Azuma, J., and Kosijimi, T. (1984) *Holzforschung* 38, 141–149.

37. Fukushima, K., and Terashima, N. (1989) *J. Wood Chem. Technol.* 10, 413–438.

38. Ruel, K., Faix, O., and Joseleau, J. P. (1994) *J. Trace Microprobe Tech.* 12, 247–265.

39. Jakobsons, J., Gravitis, J., and Dashevskii, V. G. (1982) *Zh. Strukt. Khim.* 23, 74–82.